

## Supplementary Materials for

### Controlling fluid-induced seismicity during a 6.1-km-deep geothermal stimulation in Finland

Grzegorz Kwiatek\*, Tero Saarno, Thomas Ader, Felix Bluemle, Marco Bohnhoff, Michael Chendorain, Georg Dresen, Pekka Heikkinen, Ilmo Kukkonen, Peter Leary, Maria Leonhardt, Peter Malin, Patricia Martínez-Garzón, Kevin Passmore, Paul Passmore, Sergio Valenzuela, Christopher Wollin

\*Corresponding author. Email: kwiatek@gfz-potsdam.de

Published 1 May 2019, *Sci. Adv.* **5**, eaav7224 (2019)

DOI: 10.1126/sciadv.aav7224

#### This PDF file includes:

Fig. S1. Location of St1 Deep Heat Oy project site and different seismic networks used to monitor the stimulation campaign.

Fig. S2. Optimized velocity model for P and S waves (black and red lines, respectively), initially compiled from borehole logs.

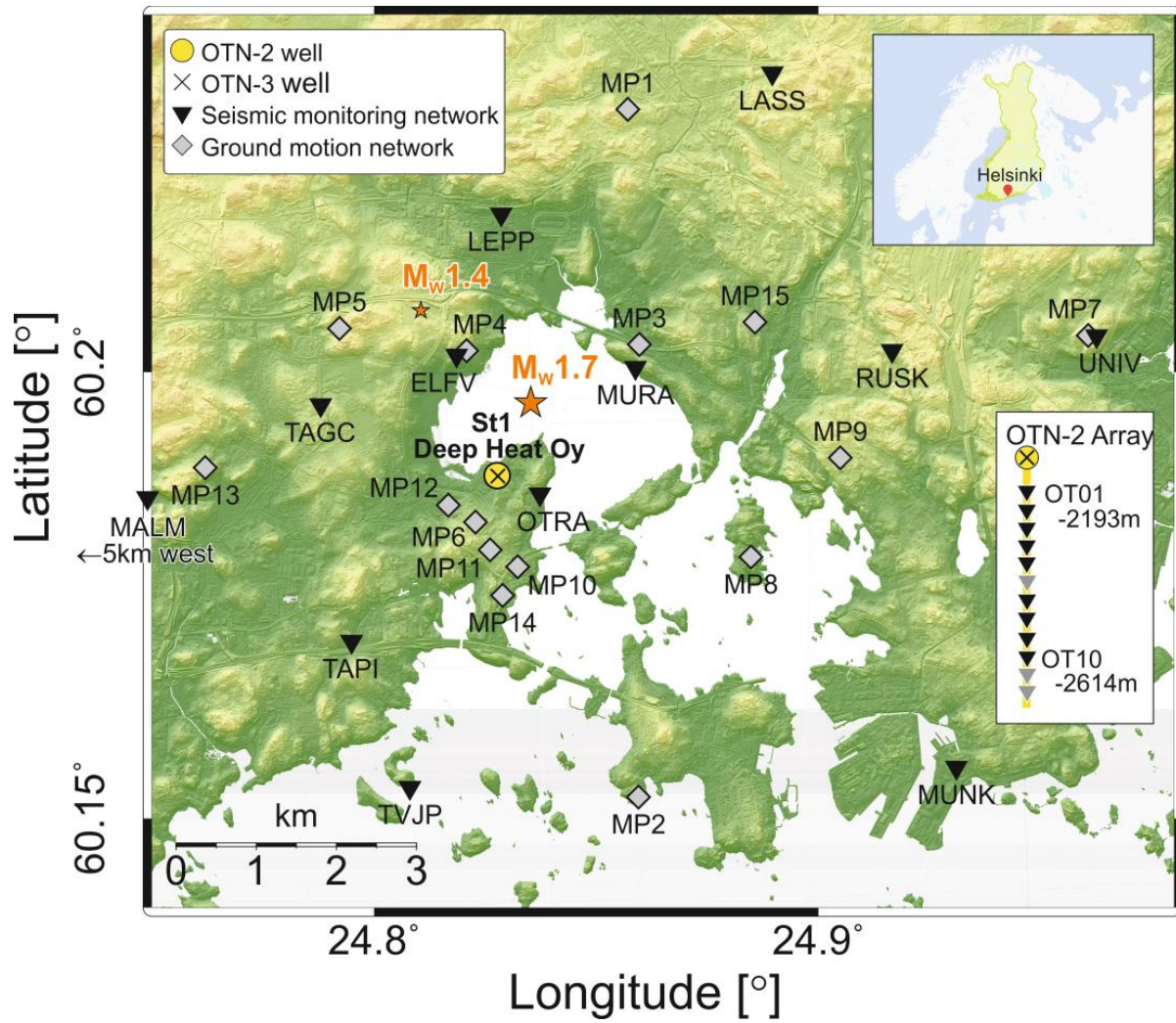
Fig. S3. Key time intervals indicating changes in pumping protocols (Roman numerals) together with pressure and cumulative injection per injection subphase (see Materials and Methods for detailed description of changes in pumping protocol).

Fig. S4.  $b$ -value distribution for the full catalog.

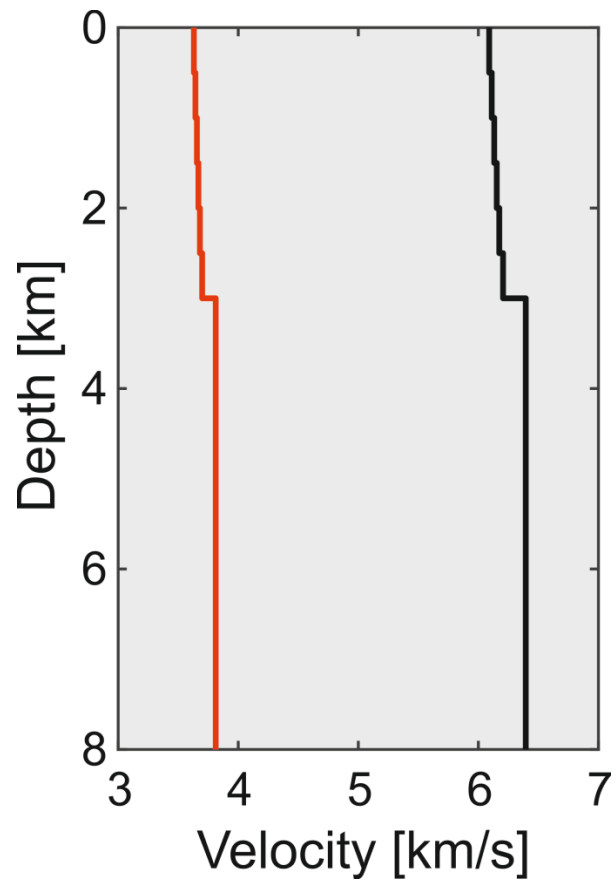
Fig. S5. Results of declustering analysis.

Fig. S6. Dependence between corner frequency and seismic moment for the group of 56 earthquakes with  $M_W$  between 0.9 and 1.9, for which spectral parameters have been estimated using the spectral fitting method.

Text S1. Access to catalog data



**Fig. S1. Location of St1 Deep Heat Oy project site and different seismic networks used to monitor the stimulation campaign.** Two natural earthquakes that occurred in 2011 in the proximity of project site are shown as orange stars.



**Fig. S2. Optimized velocity model for P and S waves (black and red lines, respectively), initially compiled from borehole logs.**

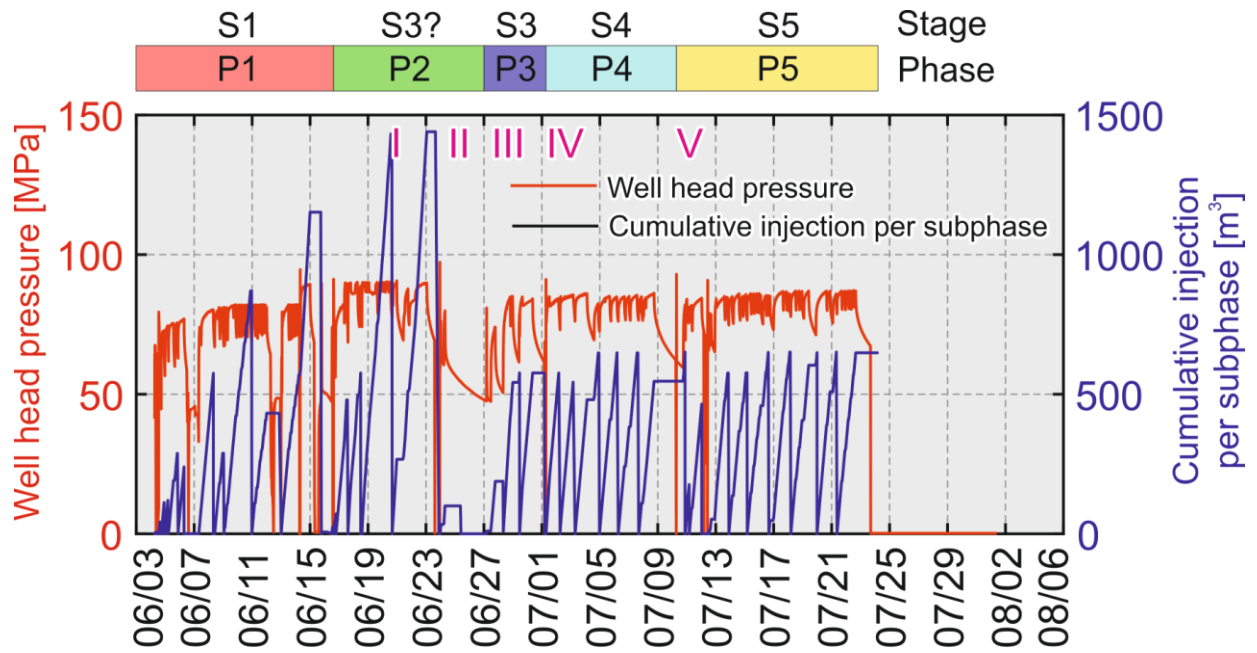


**Fig. S3. Key time intervals indicating changes in pumping protocols (Roman numerals) together with pressure and cumulative injection per injection subphase (see Materials and Methods for detailed description of changes in pumping protocol).**

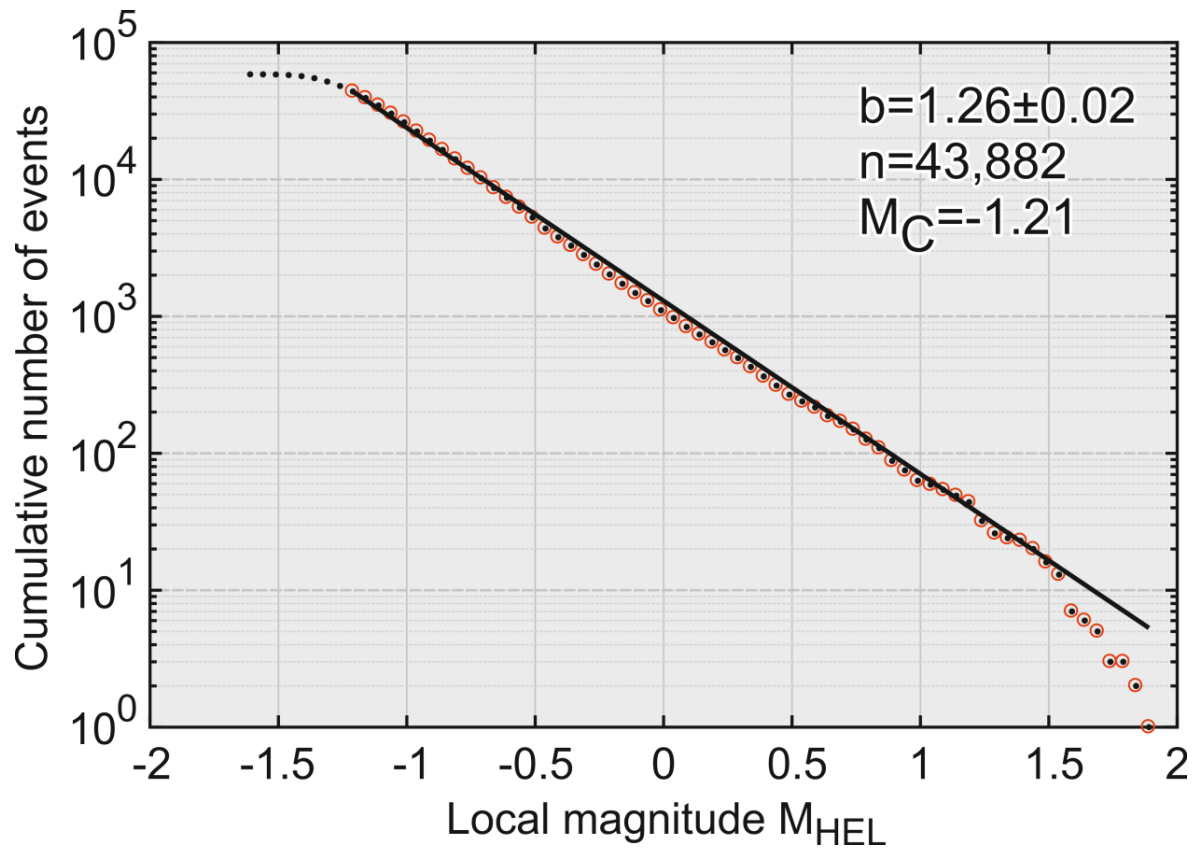
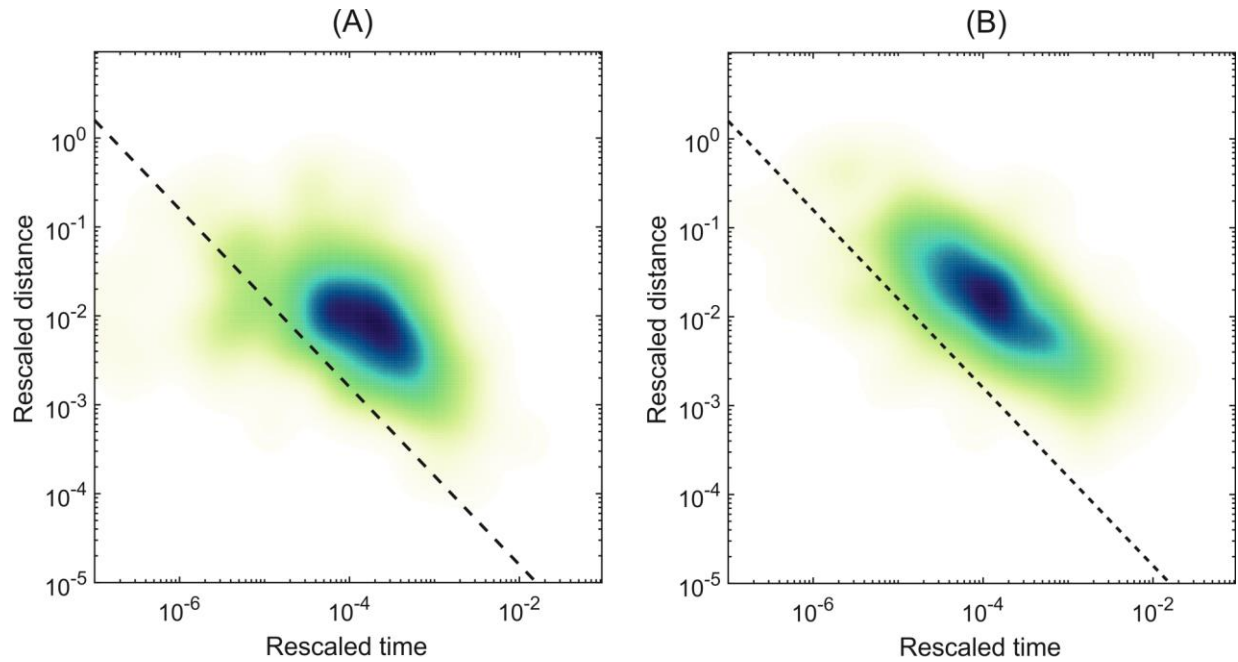
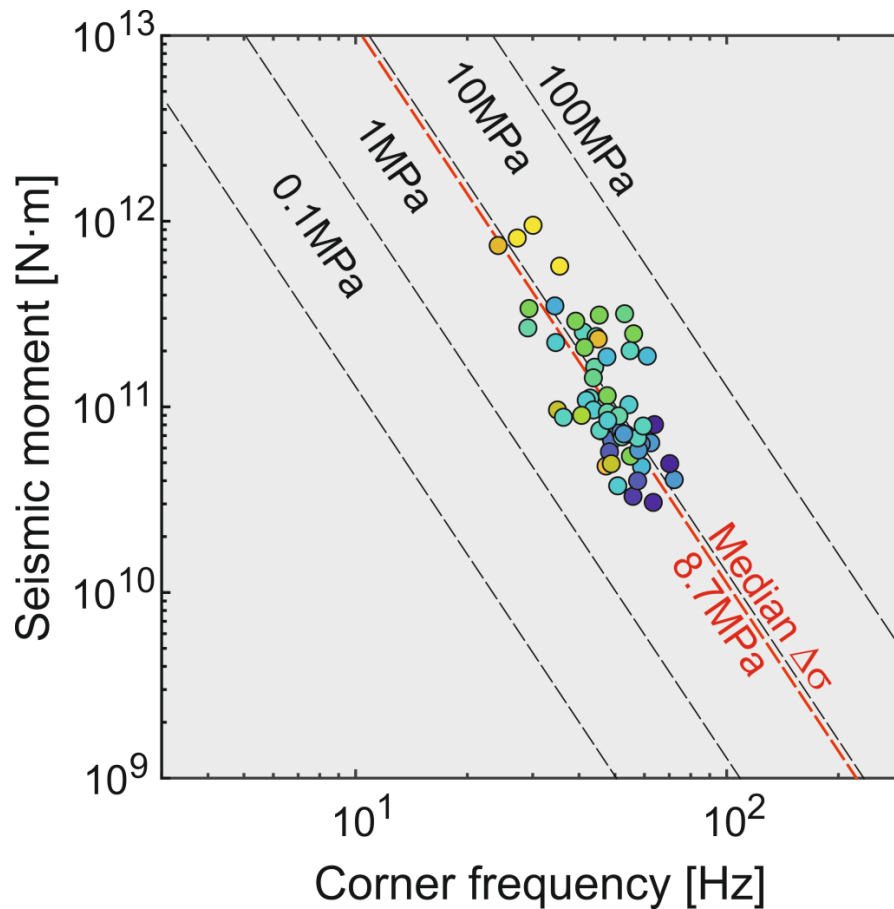


Fig. S4. *b*-value distribution for the full catalog.



**Fig. S5. Results of declustering analysis.** Distribution of rescaled inter-event time – inter-event distance for original relocated catalog (A) and its reshuffled version (B), where the relations between inter-event times, distances and magnitudes have been destroyed. The dashed line was selected using the reshuffled catalog, leading to separation of the catalog into 88% of background and 12% of clustered earthquakes.



**Fig. S6. Dependence between corner frequency and seismic moment for the group of 56 earthquakes with  $M_W$  between 0.9 and 1.9, for which spectral parameters have been estimated using the spectral fitting method.** The lines of constant stress drop ranging 0.1-100 MPa are painted assuming the circular source model of Madariaga (57).

**Text S1. Access to catalog data**

The Double-Difference relocated catalog containing  $N=1,997$  events is available through GFZ data services (30). The catalog contains ID number, origin time, location in local Cartesian coordinate system and associate uncertainties, local magnitude and event classification information (injection phase): <https://doi.org/10.5880/G0046Z.4.2.2019.001>.